

Document downloaded from:

<http://hdl.handle.net/10251/37326>

This paper must be cited as:

Giménez Pastor, A.; Ihab Alkhoury; Andrés Ferrer, J.; Juan Císcar, A. (2014). Handwriting word recognition using windowed Bernoulli HMMs. *Pattern Recognition Letters*. 35:149-156. doi:10.1016/j.patrec.2012.09.002.



The final publication is available at

<http://dx.doi.org/10.1016/j.patrec.2012.09.002>

Copyright Elsevier

# Handwriting word recognition using windowed Bernoulli HMMs

Adrià Giménez, Ihab Khoury, Jesús Andrés-Ferrer and Alfons Juan  
*DSIC/ITI, Universitat Politècnica de València, Camí de Vera s/n, 46022 València, Spain*

---

## Abstract

Hidden Markov Models (HMMs) are now widely used for off-line handwriting recognition in many languages. As in speech recognition, they are usually built from shared, embedded HMMs at symbol level, where state-conditional probability density functions in each HMM are modeled with Gaussian mixtures. In contrast to speech recognition, however, it is unclear which kind of features should be used and, indeed, very different features sets are in use today. Among them, we have recently proposed to directly use columns of raw, binary image pixels, which are directly fed into embedded Bernoulli (mixture) HMMs, that is, embedded HMMs in which the emission probabilities are modeled with Bernoulli mixtures. The idea is to by-pass feature extraction and to ensure that no discriminative information is filtered out during feature extraction, which in some sense is integrated into the recognition model. In this work, column bit vectors are extended by means of a sliding window of adequate width to better capture image context at each horizontal position of the word image. Using these *windowed* Bernoulli mixture HMMs,

---

*Email address:* {agimenez,ialkhoury,jandres,ajuan}@dsic.upv.es (Adrià Giménez, Ihab Khoury, Jesús Andrés-Ferrer and Alfons Juan)

good results are reported on the well-known IAM and RIMES databases of Latin script, and in particular, state-of-the-art results are provided on the IfN/ENIT database of Arabic handwritten words.

*Keywords:* HTR, Bernoulli HMM, Latin, Arabic, Sliding window

---

## 1. Introduction

Hidden Markov Models (HMMs) are now widely used for off-line handwriting recognition in many languages and, in particular, in languages with Latin and Arabic scripts (Dehghan et al., 2001; Günter and Bunke, 2004; Märgner and El Abed, 2007, 2009; Grosicki and El Abed, 2009). Following the conventional approach in speech recognition (Rabiner and Juang, 1993), HMMs at global (line or word) level are built from shared, *embedded* HMMs at character (subword) level, which are usually simple in terms of number of states and topology. In the common case of real-valued feature vectors, state-conditional probability (density) functions are modeled as Gaussian mixtures since, as with finite mixture models in general, their complexity can be easily adjusted to the available training data by simply varying the number of components.

After decades of research in speech recognition, the use of certain real-valued speech features and embedded Gaussian (mixture) HMMs is a de-facto standard (Rabiner and Juang, 1993). However, in the case of handwriting recognition, there is no such a standard and, indeed, very different sets of features are in use today. In Giménez and Juan (2009) we proposed to bypass feature extraction and to directly feed columns of raw, binary pixels into *embedded Bernoulli (mixture) HMMs (BHMMs)*, that is, embedded HMMs

21 in which the emission probabilities are modeled with Bernoulli mixtures. The  
22 basic idea is to ensure that no discriminative information is filtered out during  
23 feature extraction, which in some sense is integrated into the recognition  
24 model. In Giménez et al. (2010), we improved our basic approach by using  
25 a sliding window of adequate width to better capture image context at each  
26 horizontal position of the text image. This improvement, to which we refer  
27 as *windowed BHMMs*, achieved very competitive results on the well-known  
28 IfN/ENIT database of Arabic town names (Pechwitz et al., 2002).

29 Although windowed BHMMs achieved good results on IfN/ENIT, it was  
30 clear to us that text distortions are more difficult to model with wide windows  
31 than with narrow (e.g. one-column) windows. In order to circumvent this dif-  
32 ficulty, we have considered new, adaptative window sampling techniques, as  
33 opposed to the conventional, direct strategy by which the sampling window  
34 center is applied at a constant height of the text image and moved horizon-  
35 tally one pixel at a time. More precisely, these adaptative techniques can  
36 be seen as an application of the direct strategy followed by a *repositioning*  
37 step by which the sampling window is repositioned to align its center to the  
38 center of gravity of the sampled image. This repositioning step can be done  
39 horizontally, vertically or in both directions. Although vertical repositioning  
40 was expected to have more influence on recognition results than horizontal  
41 repositioning, we decided to study both separately, and also in conjunction,  
42 so as to confirm this expectation.

43 In this paper, the repositioning techniques described above are introduced  
44 and extensively tested on different, well-known databases for off-line hand-  
45 writing recognition. In particular, we provide new, state-of-the-art results on

46 the IfN/ENIT database, which clearly outperform our previous results with-  
 47 out repositioning (Giménez et al., 2010). Indeed, the first tests on IfN/ENIT  
 48 of our windowed BHMM system with vertical repositioning were made at the  
 49 ICFHR 2010 Arabic Handwriting Recognition Competition, where our sys-  
 50 tem ranked first (Märgner and El Abed, 2010). Moreover, the test sets used  
 51 in this competition were also used in a new competition at the ICDAR 2011  
 52 and none of the participants improved the results achieved by our system at  
 53 the ICFHR 2010 conference (Märgner and El Abed, 2011). Apart from state-  
 54 of-the-art results on IfN/ENIT, we also provide new empirical results on the  
 55 IAM database of English words (Marti and Bunke, 2002) and the RIMES  
 56 database of French words (Grosicki et al., 2009). Our windowed BHMM  
 57 system with vertical repositioning achieves good results on both databases.

58 In what follows, we briefly review Bernoulli mixtures (Sec. 2), BHMMs  
 59 (Sec. 3), maximum likelihood parameter estimation (Sec. 4) and *windowed*  
 60 *BHMMs* repositioning techniques (Sec. 5). Empirical results are then re-  
 61 ported in Sec. 6 and concluding remarks are given in Sec. 7.

## 62 2. Bernoulli Mixture

63 Let  $\mathbf{o}$  be a  $D$ -dimensional feature vector. A finite mixture is a probability  
 64 (density) function of the form:

$$P(\mathbf{o} | \Theta) = \sum_{k=1}^K \pi_k P(\mathbf{o} | k, \Theta_k), \quad (1)$$

65 where  $K$  is the number of mixture components,  $\pi_k$  is the  $k$ -th component  
 66 coefficient, and  $P(\mathbf{o} | k, \Theta_k)$  is the  $k$ -th component-conditional probability  
 67 (density) function. The mixture is controlled by a parameter vector  $\Theta$  com-

68 prising the mixture coefficients and a parameter vector for the components,  
 69  $\Theta_k$ . It can be seen as a generative model that first selects the  $k$ -th component  
 70 with probability  $\pi_k$  and then generates  $\mathbf{o}$  in accordance with  $P(\mathbf{o} | k, \Theta_k)$ .

71 A Bernoulli mixture model is a particular case of (1) in which each com-  
 72 ponent  $k$  has a  $D$ -dimensional Bernoulli probability function governed by its  
 73 own vector of parameters or *prototype*  $\mathbf{p}_k = (p_{k1}, \dots, p_{kD})^t \in [0, 1]^D$ ,

$$P(\mathbf{o} | k, \Theta_k) = \prod_{d=1}^D p_{kd}^{o_d} (1 - p_{kd})^{1-o_d}, \quad (2)$$

74 where  $p_{kd}$  is the probability for bit  $d$  to be 1. Note that this equation is just  
 75 the product of independent, unidimensional Bernoulli probability functions.  
 76 Therefore, for a fixed  $k$ , it can not capture any kind of dependencies or  
 77 correlations between individual bits.

### 78 3. Bernoulli HMM

79 Let  $O = (\mathbf{o}_1, \dots, \mathbf{o}_T)$  be a sequence of feature vectors. An HMM is a  
 80 probability (density) function of the form:

$$P(O | \Theta) = \sum_{q_1, \dots, q_T} \prod_{t=0}^T a_{q_t q_{t+1}} \prod_{t=1}^T b_{q_t}(\mathbf{o}_t), \quad (3)$$

81 where the sum is over all possible *paths* (state sequences)  $q_0, \dots, q_{T+1}$ , such  
 82 that  $q_0 = I$  (special *initial* or *start* state),  $q_{T+1} = F$  (special *final* or *stop*  
 83 state), and  $q_1, \dots, q_T \in \{1, \dots, M\}$ , being  $M$  the number of regular (non-  
 84 special) states of the HMM. On the other hand, for any regular states  $i$  and  $j$ ,  
 85  $a_{ij}$  denotes the *transition* probability from  $i$  to  $j$ , while  $b_j$  is the *observation*  
 86 probability (density) function at  $j$ .

87 A Bernoulli (mixture) HMM (BHMM) is an HMM in which the probabil-  
 88 ity of observing the binary feature vector  $\mathbf{o}_t$ , when  $q_t = j$ , follows a Bernoulli  
 89 mixture distribution for the state  $j$

$$b_j(\mathbf{o}_t) = \sum_{k=1}^K \pi_{jk} \prod_{d=1}^D p_{jkd}^{o_{td}} (1 - p_{jkd})^{1-o_{td}}, \quad (4)$$

90 where  $o_{td}$  is the  $d$ -th bit of  $\mathbf{o}_t$ ,  $\pi_{jk}$  is the prior of the  $k$ -th mixture component  
 91 in state  $j$ , and  $p_{jkd}$  is the probability that this component assigns to  $o_{td}$  to  
 92 be 1.

93 Consider the upper part of Fig. 1, where a BHMM example for the num-  
 94 ber 3 is shown, together with a binary image generated from it. It is a  
 95 three-state model with single prototypes attached to states 1 and 2, and a  
 96 two-component mixture assigned to state 3, where Bernoulli prototypes are  
 97 depicted as a gray image (black=1, white=0, gray=0.5). It is worth noting  
 98 that prototypes do not account for the whole digit realizations, but only for  
 99 single columns. This column-by-column emission of feature vectors attempts  
 100 to better model horizontal distortions at character level and, indeed, it is the  
 101 usual approach in both speech and handwriting recognition when continuous-  
 102 density (Gaussian mixture) HMMs are used. The reader can check that, by  
 103 direct application of (3) and taking into account the existence of two different  
 104 state sequences, the probability of generating the binary image generated in  
 105 this example is 0.063.

106 As discussed in the introduction, BHMMs at global (line or word) level  
 107 are built from shared, embedded BHMMs at character level. More precisely,  
 108 let  $C$  be the number of different characters (symbols) from which global  
 109 BHMMs are built, and assume that each character  $c$  is modeled with a dif-

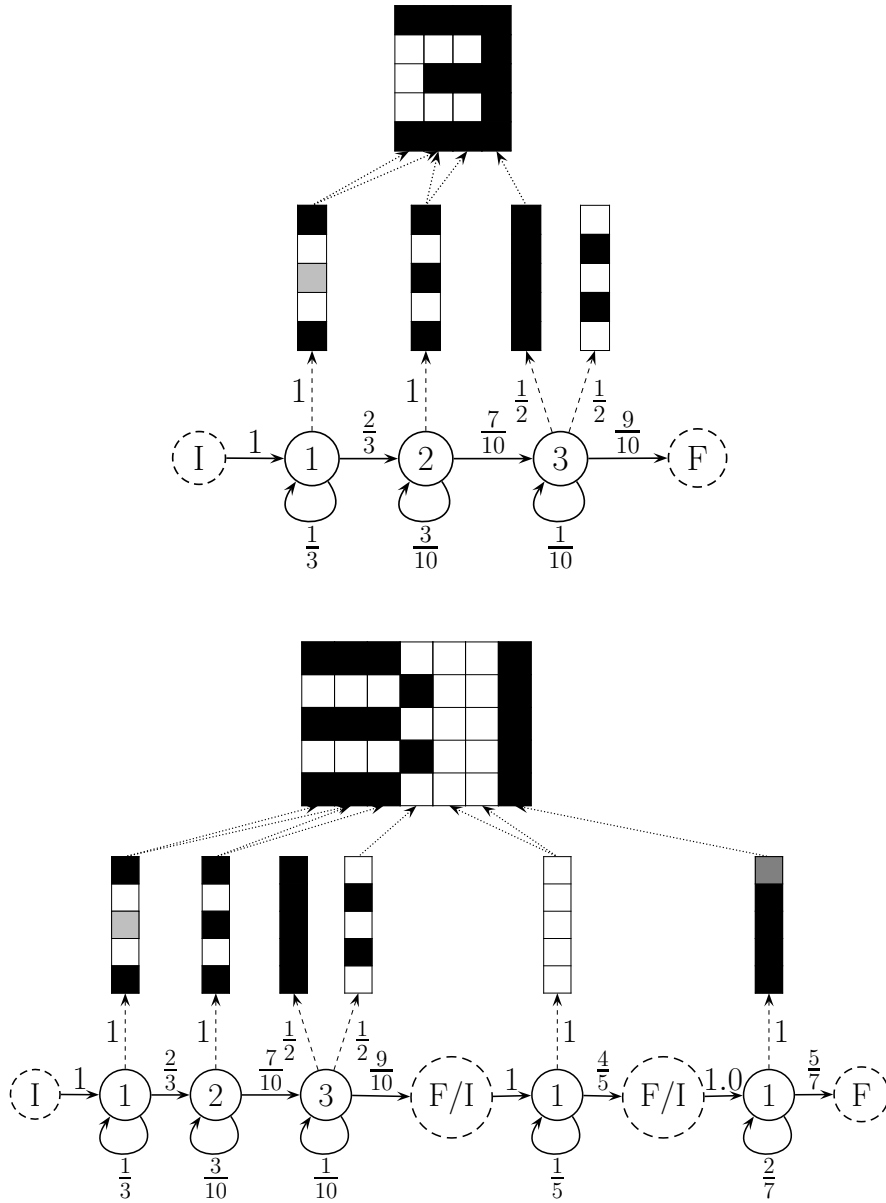


Figure 1: BHMM examples for the numbers 3 (top) and 31 (bottom), together with binary images generated from them. Note that the BHMM example for the number 3 is also embedded into the number 31 example. Bernoulli prototype probabilities are represented using the following color scheme: black=1, white=0, gray=0.5 and light gray=0.1.



110 ferent BHMM of parameter vector  $\Theta_c$ . Let  $\Theta = \{\Theta_1, \dots, \Theta_C\}$ , and let  
 111  $O = (\mathbf{o}_1, \dots, \mathbf{o}_T)$  be a sequence of feature vectors generated from a sequence  
 112 of symbols  $S = (s_1, \dots, s_L)$ , with  $L \leq T$ . The probability of  $O$  can be calcu-  
 113 lated, using embedded HMMs for its symbols, as:

$$P(O | S, \Theta) = \sum_{i_1, \dots, i_{L+1}} \prod_{l=1}^L P(\mathbf{o}_{i_l}, \dots, \mathbf{o}_{i_{l+1}-1} | \Theta_{s_l}), \quad (5)$$

114 where the sum is carried out over all possible segmentations of  $O$  into  $L$   
 115 segments, that is, all sequences of indices  $i_1, \dots, i_{L+1}$  such that

$$1 = i_1 < \dots < i_L < i_{L+1} = T + 1;$$

116 and  $P(\mathbf{o}_{i_l}, \dots, \mathbf{o}_{i_{l+1}-1} | \Theta_{s_l})$  refers to the probability (density) of the  $l$ -th  
 117 segment, as given by (3) using the HMM associated with symbol  $s_l$ .

118 Consider now the lower part of Fig. 1. An embedded BHMM for the  
 119 number 31 is shown, which is the result of concatenating BHMMs for the  
 120 digit 3, blank space and digit 1, in that order. Note that the BHMMs for  
 121 blank space and digit 1 are simpler than that for digit 3. Also note that the  
 122 BHMM for digit 3 is shared between the two embedded BHMMs shown in the  
 123 figure. The binary image of the number 31 shown above can only be generated  
 124 from two paths, as indicated by the arrows connecting prototypes to image  
 125 columns, which only differ in the state generating the second image column  
 126 (either state 1 or 2 of the BHMM for the first symbol). It is straightforward  
 127 to check that, according to (5), the probability of generating this image is  
 128 0.0004.

129 **4. Maximum Likelihood Parameter Estimation**

130 Maximum likelihood estimation (MLE) of the parameters governing an  
 131 embedded BHMM does not differ significantly from the conventional Gaus-  
 132 sian case, and it is also efficiently performed using the well-known EM (Baum-  
 133 Welch) re-estimation formulae (Rabiner and Juang, 1993; Young et al., 1995).  
 134 Let  $(O_1, S_1), \dots, (O_N, S_N)$ , be a collection of  $N$  training samples in which the  
 135  $n$ -th observation has length  $T_n$ ,  $O_n = (\mathbf{o}_{n1}, \dots, \mathbf{o}_{nT_n})$ , which corresponds to  
 136 a sequence of  $L_n$  symbols ( $L_n \leq T_n$ ),  $S_n = (s_{n1}, \dots, s_{nL_n})$ . At iteration  $r$ ,  
 137 the E step requires the computation, for each training sample  $n$ , of its corre-  
 138 sponding forward ( $\alpha$ ) and backward ( $\beta$ ) recurrences (see Rabiner and Juang  
 139 (1993)), as well as

$$z_{nltk}^{(r)}(j) = \frac{\pi_{s_{nl}jk}^{(r)} \prod_{d=1}^D p_{s_{nl}jkd}^{(r) o_{ntd}} (1 - p_{s_{nl}jkd}^{(r)})^{1-o_{ntd}}}{b_{s_{nl}j}^{(r)}(\mathbf{o}_{nt})}, \quad (6)$$

140 for each  $t, k, j, l$ . In (6),  $z_{nltk}^{(r)}(j)$  is the probability of  $\mathbf{o}_{nt}$  to be generated  
 141 in the  $k$ -th mixture component, given that  $\mathbf{o}_{nt}$  has been generated in the  
 142  $j$ -th state of symbol  $s_l$ . The conditional probability function  $b_{s_{nl}j}^{(r)}(\mathbf{o}_{nt})$  is  
 143 analogous to that defined in (4).

144 In the M step, the Bernoulli prototype corresponding to the  $k$ -th compo-  
 145 nent of the state  $j$  for character  $c$  has to be updated as

$$\mathbf{p}_{cjk}^{(r+1)} = \frac{1}{\gamma_{ck}(j)} \sum_n \frac{\sum_{l:s_{nl}=c} \sum_{t=1}^{T_n} \xi_{nltk}^{(r)}(j) \mathbf{o}_{nt}}{P(O_n | S_n, \Theta^{(r)})}, \quad (7)$$

146 where  $\gamma_{ck}(j)$  is a normalization factor

$$\gamma_{ck}(j) = \sum_n \frac{\sum_{l:s_{nl}=c} \sum_{t=1}^{T_n} \xi_{nltk}^{(r)}(j)}{P(O_n | S_n, \Theta^{(r)})}, \quad (8)$$

147 and  $\xi_{nltk}^{(r)}(j)$  is the probability of  $O_n$  when the  $t$ -th feature vector of the  $n$ -th  
 148 sample corresponds to symbol  $s_l$  and is generated by the  $k$ -th component of  
 149 the state  $j$ ,

$$\xi_{nltk}^{(r)}(j) = \alpha_{nlt}^{(r)}(j) z_{nltk}^{(r)}(j) \beta_{nlt}^{(r)}(j). \quad (9)$$

150 Similarly, the  $k$ -th component coefficient of the state  $j$  in the HMM for  
 151 character  $c$  is updated by

$$\pi_{cjk}^{(r+1)} = \frac{1}{\gamma_c(j)} \sum_n \frac{\sum_{l:s_{nl}=c} \sum_{t=1}^{T_n} \xi_{nltk}^{(r)}(j)}{P(O_n | S_n, \Theta^{(r)})}, \quad (10)$$

152 where  $\gamma_c(j)$  is a normalization factor

$$\gamma_c(j) = \sum_n \frac{\sum_{l:s_{nl}=c} \sum_{t=1}^{T_n} \alpha_{nlt}^{(r)}(j) \beta_{nlt}^{(r)}(j)}{P(O_n | S_n, \Theta^{(r)})}. \quad (11)$$

153 Finally, it is well-known that MLE tends to overtrain the models. In  
 154 order to amend this problem Bernoulli prototypes are smoothed by linear  
 155 interpolation with a flat (uniform) prototype, **0.5**,

$$\tilde{\mathbf{p}} = (1 - \delta) \mathbf{p} + \delta \mathbf{0.5}, \quad (12)$$

156 where  $\delta$  is usually optimized in a validation set or fixed to a sensible value  
 157 such as  $\delta = 10^{-6}$

## 158 5. Windowed BHMMs

159 Given a binary image normalized in height to  $H$  pixels, we may think of a  
 160 feature vector  $\mathbf{o}_t$  as its column at position  $t$  or, more generally, as a concate-  
 161 nation of columns in a window of  $W$  columns in width, centered at position

162 *t*. This generalization has no effect neither on the definition of BHMM nor  
163 on its MLE, although it would be very helpful to better capture the image  
164 context at each horizontal position of the image. As an example, Fig. 2  
165 shows a binary image of 4 columns and 5 rows, which is transformed into  
166 a sequence of four 15-dimensional feature vectors (first row) by application  
167 of a sliding window of width 3. For clarity, feature vectors are depicted as  
168  $3 \times 5$  subimages instead of 15-dimensional column vectors. Note that feature  
169 vectors at positions 2 and 4 would be indistinguishable if, as in our previous  
170 approach, they were extracted with no context ( $W = 1$ ).

171 Although one-dimensional, “horizontal” HMMs for image modeling can  
172 properly capture non-linear horizontal image distortions, they are somewhat  
173 limited when dealing with vertical image distortions, and this limitation  
174 might be particularly strong in the case of feature vectors extracted with  
175 significant context. To overcome this limitation, we have considered three  
176 methods of window *repositioning* after window extraction: *vertical*, *horizon-*  
177 *tal*, and *both*. The basic idea is to first compute the center of mass of the  
178 extracted window, which is then repositioned (translated) to align its center  
179 to the center of mass. This is done in accordance with the chosen method,  
180 that is, horizontally, vertically, or in both directions. Obviously, the feature  
181 vector actually extracted is that obtained after repositioning. An example  
182 of feature extraction is shown in Fig. 2 in which the standard method (no  
183 repositioning) is compared with the three methods repositioning methods  
184 considered.

185 It is helpful to observe the effect of the repositioning with real data. Fig. 3  
186 shows the sequence of feature vectors extracted from a real sample of the

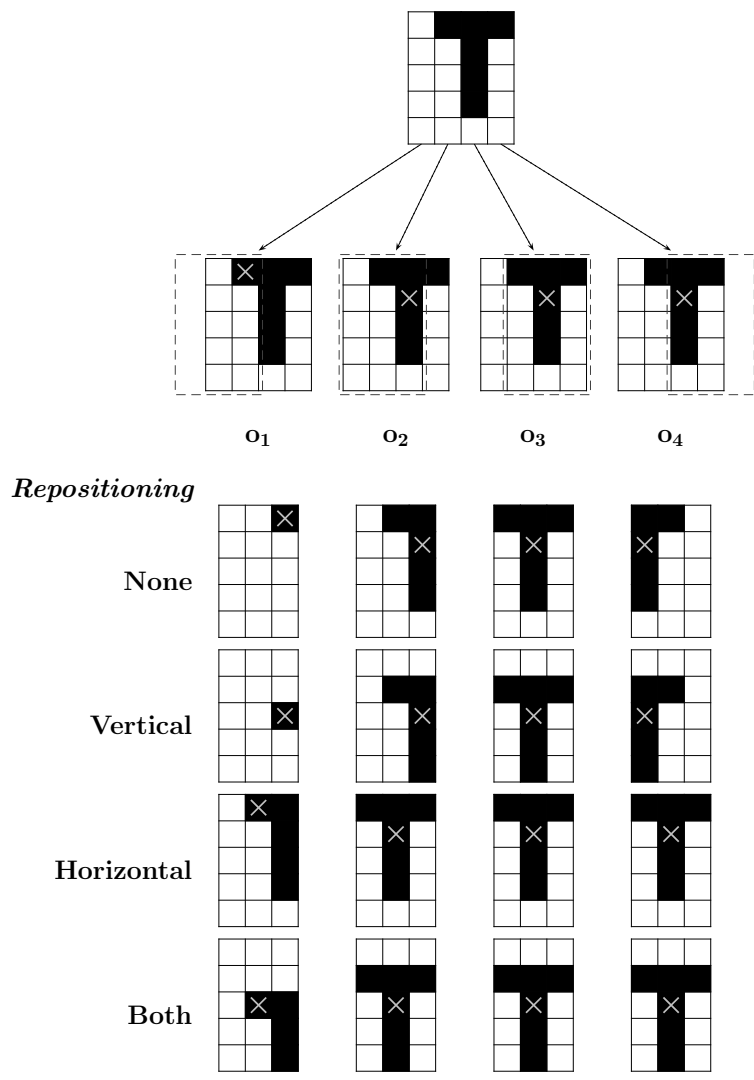


Figure 2: Example of transformation of a  $4 \times 5$  binary image (top) into a sequence of 4 15-dimensional binary feature vectors  $O = (\mathbf{o}_1, \mathbf{o}_2, \mathbf{o}_3, \mathbf{o}_4)$  using a window of width 3. After window extraction (illustrated under the original image), the standard method (no repositioning) is compared with the three repositioning methods considered: vertical, horizontal, and both directions. Mass centers of extracted windows are also indicated.

187 IFN/ENIT database, with and without (both) repositioning. As intended,  
 188 (vertical or both) repositioning has the effect of normalizing vertical image  
 189 distortions, especially translations.

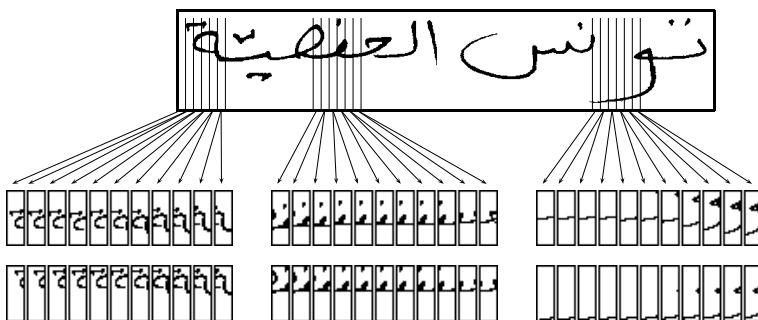


Figure 3: Original sample *pf069\_011* from IFN/ENIT database (top) and its sequence of feature vectors produced with and without (both) repositioning (center and bottom, respectively).

## 190 6. Experiments

191 Our windowed BHMMs and the repositioning techniques described above  
 192 were tested on three well-known databases of handwritten words: the IfN/ENIT  
 193 database (Pechwitz et al., 2002), IAM words (Marti and Bunke, 2002) and  
 194 RIMES (Grosicki et al., 2009). In what follows, we describe experiments and  
 195 results in each database separately.

### 196 6.1. IfN/ENIT

197 The IfN/ENIT database of Arabic handwritten Tunisian town names  
 198 is a widely used database to compare Arabic handwriting recognition sys-  
 199 tems (Pechwitz et al., 2002). As in the Arabic handwriting recognition com-  
 200 petition held at ICDAR in 2007 (Märgner and El Abed, 2007), we used

201 IfN/ENIT version 2.0, patch level 1e (v2.0p1e). It comprises 32492 Arabic  
202 word images written by more than 1000 different writers, from a lexicon of  
203 937 Tunisian town/village names. For the experiments reported below, each  
204 image was first rescaled in height to  $D = 30$  rows, while keeping the original  
205 aspect ratio, and then binarized using Otsu’s binarization method. The re-  
206 sulting set of binary images was partitioned into five folds labeled as a, b, c,  
207 d and e, as defined in (Märgner and El Abed, 2007).

208 In a first series of experiments, we tried different values for the sliding  
209 window width  $W$  (1, 3, 5, 7, 9 and 11) and also different values for number of  
210 mixture components per state  $K$  (1, 2, 4, 8, 16, 32, 64). However, taking into  
211 account our previous, preliminary results in Khoury et al. (2010), we only  
212 tried BHMMs with 6 states as character models. For  $K = 1$ , BHMMs were  
213 initialized by first segmenting the training set with a “neutral” model anal-  
214 ogous to that in Young et al. (1995), and then using the resulting segments  
215 to perform a Viterbi initialization. For  $K > 1$ , BHMMs were initialized by  
216 splitting the mixture components of the models trained with  $K/2$  mixture  
217 components per state. In each case, 4 EM iterations were run after initial-  
218 ization. As usual with conventional HMM systems (Young et al., 1995), the  
219 Viterbi algorithm was used in combination with a table of prior probabilities  
220 so as to find the most probable transcription (class) of each test image.

221 Fig. 4 (top) shows the Word Error Rate (WER%) as a function of the  
222 number of mixture components, for varying sliding window widths. Each  
223 WER estimate (plotted point) was obtained by cross-validation with the first  
224 4 standard folds (abcd). It is clear that the use of sliding windows improves  
225 the results to a large extent. Specifically, the best result, 7.4%, is obtained

226 for  $W = 9$  and  $K = 32$ , although very similar results are obtained for  $W = 7$   
227 and  $W = 11$ . It is worth noting that the best result achieved with no sliding  
228 windows ( $W = 1$ ) is 17.7%, that is, 10 absolute points above of the best  
229 result achieved with sliding windows.

230 For better understanding of BHMM character models, the model for char-  
231 acter  $\dot{\text{خ}}$ , trained from folds abc with  $W = 9$  and  $K = 32$ , is (partially) de-  
232 picted in Fig. 5 (top) together with its Viterbi alignment with a real image  
233 of the character  $\dot{\text{خ}}$  drawn from sample *de05\_007*. As in Fig. 1 (bottom),  
234 Bernoulli prototypes are represented as gray images where the gray level of  
235 each pixel represents the probability of its corresponding pixel to be black  
236 (white = 0 and black = 1). From these prototypes, it can be seen that each  
237 state from right to left accounts for a different local part of  $\dot{\text{خ}}$ , as if the sliding  
238 window was moving smoothly from right to left. Also, note that the main  
239 stroke of the character  $\dot{\text{خ}}$  appears almost neatly drawn in most prototypes,  
240 whereas its upper dot appears blurred, probably due to a comparatively  
241 higher variability in window position.

242 Following previous results in Khoury et al. (2010), in the first series of  
243 experiments discussed above we only tried BHMMs with 6 states. However,  
244 in a recent work by Dreuw et al. (2009) where conventional (Gaussian) HMMs  
245 are tested on IfN/ENIT, the authors claim that Arabic script might be better  
246 modeled with character HMMs of variable number of states since Arabic  
247 letters are highly variable in length (as opposed to Latin letters). In order to  
248 check this claim, experiments similar to those described above were repeated  
249 with character BHMMs of different number of states. To decide on the  
250 number of states of each character BHMM, we first trained BHMMs of 4



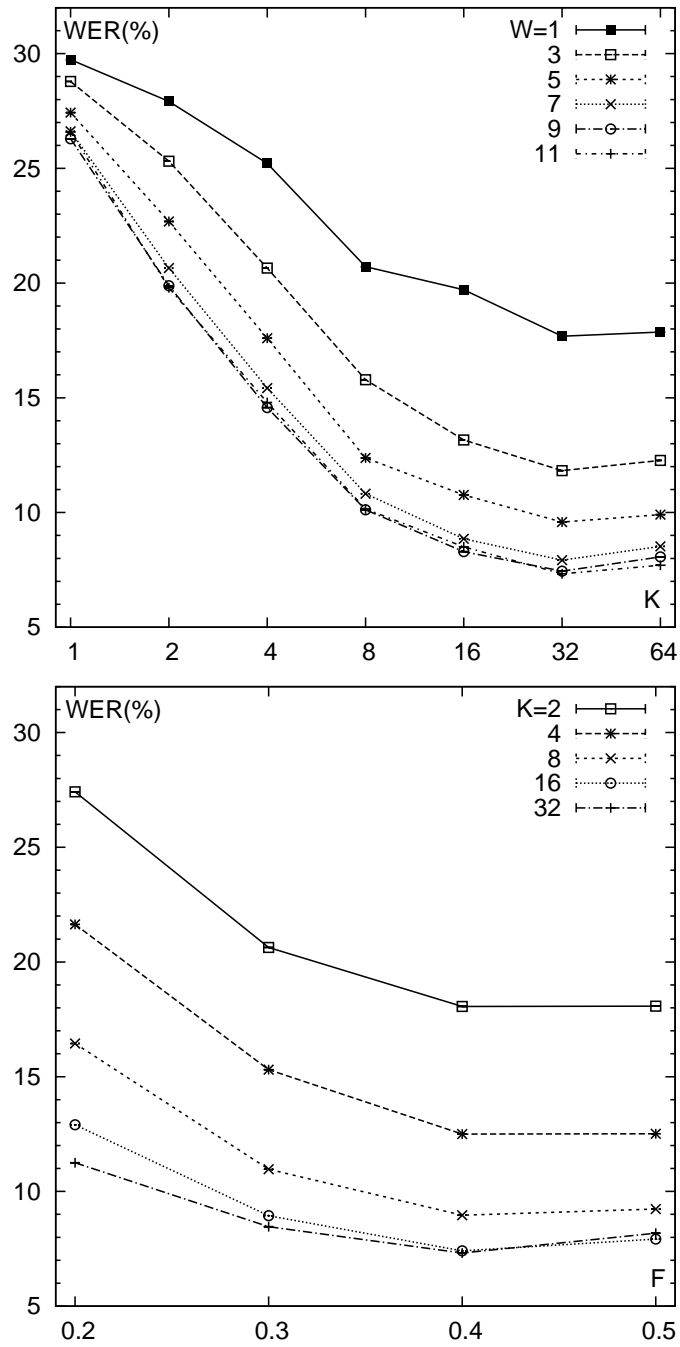


Figure 4: WER(%) on IfN/ENIT as a function of: the number of mixture components ( $K$ ) for several sliding window widths ( $W$ ) (top); and the factor  $F$  for varying values of the number of mixture components ( $K$ ) (bottom).

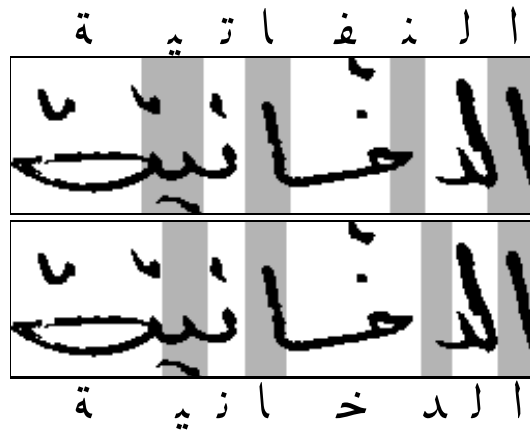
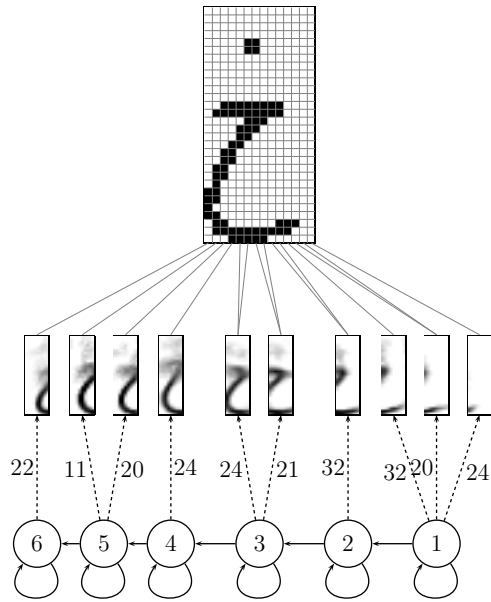


Figure 5: Top: BHMM for character خ, trained from folds abc with  $W = 9$  and  $K = 32$ , together with its Viterbi alignment with a real image of the character خ, drawn from sample *de05\_007*. Bottom: the sample *dm33\_037* is incorrectly recognized as النفاتية with BHMMs of 6 states, but correctly recognized as الدخاننية with BHMMs of variable number of states; the background color is used to represent Viterbi alignments at character level.

251 states which were then used to segment each training sample by the Viterbi  
 252 algorithm. For each character  $c$ , its average length  $\bar{T}_c$  was computed over all  
 253 occurrences of  $c$  in the segmented training data. Then, its number of states  
 254 was set to  $F \cdot \bar{T}_c$ , where  $F$  is a *factor* measuring the average number of states  
 255 that are required to emit a feature vector. The inverse of  $F$ ,  $\frac{1}{F}$  is easily  
 256 understood since it can be interpreted as a *state load*, that is, the average  
 257 number of feature vectors that are emitted in each state. For instance, a  
 258 factor of  $F = 0.2$  implies that only a fraction of 0.2 states is required to emit  
 259 a feature vector or, alternatively, that  $\frac{1}{0.2} = 5$  feature vectors are emitted on  
 260 average in each state.

261 Fig. 4 (bottom) shows the WER as a function of the factor  $F$ , for different  
 262 number of mixture components  $K$  and a window width of  $W = 9$  (with which  
 263 we obtained the best results in the previous experiments). The best result  
 264 now, 7.3% (obtained with  $F = 0.4$  and  $K = 32$ ), is similar to the 7.4%  
 265 obtained with 6 states per character. Therefore, in our case, the use of  
 266 character models of different number of states does not lead to a significant  
 267 improvement of the results.

268 Although the results with variable number of states do not lead to signif-  
 269 icant improvements, it is interesting to see that there are cases in which, as  
 270 expected, Arabic letters are better modeled with them. An example is shown  
 271 in Fig. 5 (bottom) using the sample *dm33-037*. This sample was recognized  
 272 using BHMMs with  $W = 9$ ,  $K = 32$  and both, 6 states (top) and variable  
 273 number of states with  $F = 0.4$  (bottom). In both cases, the recognized word  
 274 is Viterbi-aligned at character level (background color). Although it was in-  
 275 correctly recognized as النفاية with BHMMs of 6 states (top), it was correctly

276 recognized as الدخانية with BHMMs of variable number of states (bottom).  
 277 Note that there are two letters, 'د' and 'د', that are written at the same ver-  
 278 tical position (or column) and thus it is very difficult for our BHMMs to  
 279 recognize them as two different letters. Anyhow, the incorrectly recognized  
 280 word (top) is actually not very different in shape from the correct one; e.g.  
 281 the characters 'د' and 'د' are very similar.

282 As indicated in the introduction, this work is largely motivated by the  
 283 development of window repositioning techniques to deal with text distortions  
 284 that are difficult to model with our windowed BHMMs. To test these tech-  
 285 niques on IfN/ENIT, we used the best settings found above, that is,  $W = 9$ ,  
 286  $K = 32$  and BHMMs of variable number of states with  $F = 0.4$ . We com-  
 287 pared the standard technique (no repositioning) with the three repositioning  
 288 techniques introduced in this work: vertical, horizontal and both directions  
 289 (see Sec. 5). Results are given in Table 1 for each of the four partitions  
 290 considered above (abc-d, abd-c, acd-b, and bcd-a) and the partition abcd-e,  
 291 which is also often used by other authors.

Table 1: WER% on five IfN/ENIT partitions of four repositioning techniques: none (no repositioning), vertical, horizontal and both. We used  $W = 9$  and BHMMs of variable number of states ( $F = 0.4$ ) and  $K = 32$ .

Training	Test	None	Vertical	Horizontal	Both
abc	d	7.5	4.7	8.4	4.8
abd	c	6.9	3.6	7.7	3.8
acd	b	7.7	4.5	8.1	4.4
bcd	a	7.6	4.4	8.2	4.6
<b>abcd</b>	<b>e</b>	<b>12.3</b>	<b>6.1</b>	<b>12.4</b>	<b>6.1</b>

292 From the figures in Table 1 it is clear that vertical window reposition-  
 293 ing significantly improves the results obtained with the standard method or  
 294 horizontal repositioning alone. To our knowledge, the result obtained for the  
 295 abcd-e partition with vertical (or both) repositioning, **6.1%**, is the best result  
 296 reported on this partition to date. Indeed, it represents a 50% relative error  
 297 reduction with respect to the 12.3% of WER obtained without repositioning  
 298 which, to our knowledge, was the best result until now. As said in the in-  
 299 troduction, our windowed BHMM system with vertical repositioning ranked  
 300 first at the ICFHR 2010 Arabic Handwriting Recognition Competition. In  
 301 Table 2 we provide the best results on the test sets *f* and *s* (only known by  
 302 the organization) from the last four competition editions (Märgner and El  
 303 Abed, 2011).

Table 2: Best results from last four editions of the Arabic Handwriting Recognition Competition. Systems are based on HMM, NN (Neural Networks) or a combination of both.

System	Technology	Conference	ACC%	
			set <i>f</i>	set <i>s</i>
Siemens	HMM	ICDAR 2007	87.22	73.94
MDLSTM	NN	ICDAR 2009	<b>93.37</b>	81.06
UPV PRHLT ( <b>This work</b> )	HMM	ICFHR 2010	92.20	<b>84.62</b>
RWTH-OCR	HMM+NN	ICDAR 2011	92.20	84.55

## 304 6.2. IAM Words

305 The IAM database comprises forms of unconstrained handwritten English  
 306 text drawn from the LOB corpus and written by a total of 657 writers. This  
 307 dataset was semi-automatically annotated to isolate text line images and

308 individual handwritten words in them, from which two main versions of the  
309 dataset were built: IAM words and IAM lines. For the results reported below,  
310 we have used IAM words on the basis of a standard protocol for IAM lines,  
311 which is a writer independent protocol comprising 6 161 lines for training,  
312 920 for validation and 2 781 for testing. Only words annotated as correctly  
313 segmented were used, which resulted in 46 956 words for training, 7 358 for  
314 validation and 19 907 words for testing. We used a closed vocabulary of  
315 10 208 words for recognition, that is, the vocabulary of all words occurring  
316 in the training, validation and test sets. Class priors were computed as a  
317 smoothed unigram language model.

318 A first series of experiments was conducted on the training and validation  
319 data so as to determine appropriate preprocessing and feature extraction op-  
320 tions. We tested different preprocessing alternatives, from no preprocessing  
321 at all to a full preprocessing method consisting of three conventional steps:  
322 gray level normalization, deslanting, and size normalization (Pastor, 2007).  
323 It is worth noting that, in this context, size normalization refers to a proce-  
324 dure for vertical size normalization of three different areas in the text line  
325 image (ascenders, text body and descenders), which of course might not be  
326 correctly located in all cases. On the other hand, feature extraction com-  
327 prised three steps: rescaling of the preprocessed image to a given height  $D$ ,  
328 binarization by Otsu’s method, and final feature extraction by application of  
329 a window of a given width  $W$  and a particular repositioning technique. We  
330 tested different values of  $D$  (30 and 40) and  $W$  (9 and 11), and also each of  
331 the four repositioning techniques discussed above.

332 The best results in our first series of experiments were obtained with a

333 two-step preprocessing including gray level normalization and deslanting, fol-  
 334 lowed by feature extraction with  $D = 40$ ,  $W = 9$  and vertical repositioning.  
 335 Using these settings, a second series of experiments was conducted on the  
 336 training and validation data in which we tested different values for the num-  
 337 ber of states  $Q$  (4, 6, 8, 10 and 12) and the number of mixture components  
 338 per state  $K$  (1, 4, 16 and 64). BHMMs were trained as described in Sec. 5  
 339 for the IfN/ENIT database. The results are shown in Fig. 6. Note that our  
 340 best result in it, 24.8%, was obtained with  $K = 64$  and  $Q = 8$ .

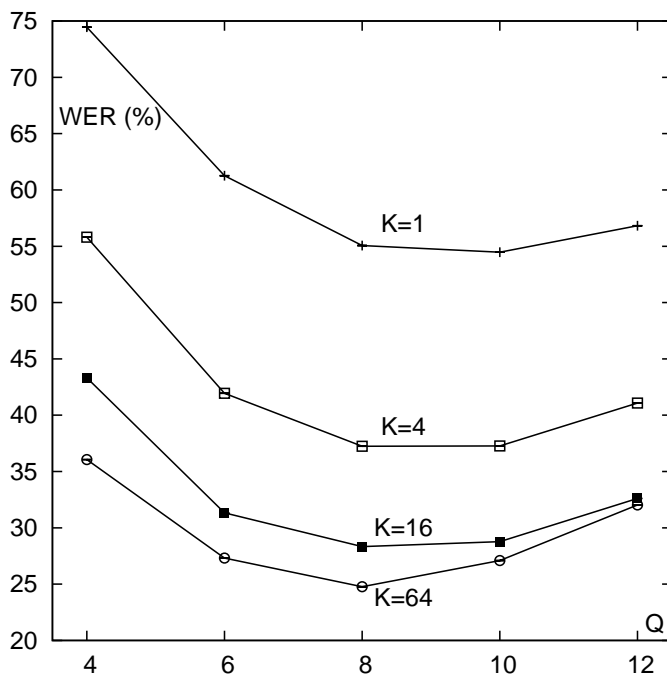


Figure 6: WER(%) on IAM words as a function of the number of states ( $Q$ ) for several number of mixture components ( $K$ ).

341 As usual in recognition of handwritten text lines, we may fine-tune sys-  
 342 tem performance by adequately weighting the importance of class priors with

Table 3: Test-set WER on IAM words obtained with BHMMs and other techniques reported in (Bianne-Bernard et al., 2011).

System	WER %
<b>BHMM (this work)</b>	25.8
Context-independent HMM (CI)	35.4
Context-dependent HMM (CD)	32.7
Combination (CI+CD+Hybrid)	21.9

343 respect to class-conditional likelihoods. This is done by introducing a *gram-*  
344 *mar scale factor*  $G$  to scale class priors. We tested several values of  $G$  on the  
345 validation set using a system trained in accordance with the best results ob-  
346 tained in the previous series of experiments. A WER of 22.4% was achieved  
347 with  $G = 90$ .

348 In our final experiment on the IAM words dataset, we trained a system  
349 on the training and validation sets, using the best settings found above for  
350 preprocessing, feature extraction and recognition. It achieved a WER of  
351 25.8% on the test set, which is quite good in comparison with other recent  
352 results on IAM words using the protocol described here (Bianne-Bernard  
353 et al., 2011). In particular, as it can be seen in Table 3, BHMMs are much  
354 better than the two systems based on HMM technology alone, though the  
355 combination of these two systems with a third, hybrid system (combining  
356 HMMs and Neural Networks) achieves even better results.

357 It must be noted that we had already tested conventional BHMMs (with  
358 one-column windows and no repositioning) on IAM words (Giménez and  
359 Juan, 2009), but we used the experimental protocol followed by Günter and



360 Bunke (2004), which is quite different to that used by Bianne-Bernard et al.  
361 (2011) and also here. Although the results are not directly comparable, our  
362 previous result with BHMMs, 29.6%, was not as good as the 25.8% of WER  
363 reported here.

### 364 6.3. RIMES

365 The *Reconnaissance et Indexation de données Manuscrites et de fac-*  
366 *similÉS* (RIMES) database of handwritten French letters was designed to  
367 evaluate automatic recognition and indexing systems of handwritten letters.  
368 Also, it has been used in several international competitions on handwritten  
369 words and line recognition (Grosicki and El Abed, 2009, 2011). For the ex-  
370 periments reported below, we have adopted the WR2 protocol used in the  
371 handwritten word recognition competition held at ICDAR 2009. It comprises  
372 44 196 samples for training, 7 542 for validation and 7 464 for testing. The  
373 lexicon to be used during recognition is that of the set to be recognized (1 636  
374 words for validation and 1 612 for testing), and the alphabet consists of 81  
375 characters. As above, class priors were computed as a smoothed unigram  
376 language model.

377 As with IAM words, a first series of experiments was conducted on the  
378 training and validation data to decide on adequate options and parameter  
379 values for preprocessing, feature extraction and recognition. In particular, we  
380 tried three preprocessing alternatives, two repositioning techniques and dif-  
381 ferent number of states ( $Q = 4, 6, 8, 10$ ) and mixture components ( $K = 1,$   
382  $4, 16$  and  $64$ ). Other parameter values used were  $D = 30$  and  $W = 9$ .  
383 The best WER, 21.7%, was obtained with a two-step preprocessing includ-  
384 ing deslanting and size normalization, followed by feature extraction with

385  $D = 30$ ,  $W = 9$  and vertical repositioning; and then BHMM trained with  
 386  $Q = 8$  and  $K = 64$ . Also as with IAM words, the performance of this system  
 387 was fine-tuned by trying several values of the grammar scale factor  $G$  on the  
 388 validation data. We achieved a WER of 18.7% with  $G = 120$ .

389 The best options and parameter values found on the validation set were  
 390 used to train a system from the training and validation data, which was finally  
 391 evaluated on the test set. We obtained a WER of 16.8%. In Table 4, this  
 392 result is compared with those reported at the ICDAR 2009 competition (using  
 393 the WR2 protocol) (Grosicki and El Abed, 2009). From these results, it  
 394 becomes clear that our windowed BHMM system with vertical repositioning  
 395 achieves comparatively good results.

Table 4: Test-set WER on RIMES obtained with BHMMs and different systems participating at the ICDAR 2009 competition (using the WR2 protocol). NN and MRF refer, respectively, to Neural Networks and Markov Random Fields.

System	Technology	WER %
TUM	NN	6.8
UPV	NN+HMM	13.9
<b>BHMM (this work)</b>	HMM	16.8
SIEMENS	HMM	18.7
ParisTech (1)	NN+HMM	19.8
IRISA	HMM	20.4
LITIS	HMM	25.9
ParisTech (2)	HMM	27.6
ParisTech (3)	HMM	36.2
ITESOFT	MRF+HMM	40.6

## 396 7. Concluding Remarks

397 Windowed Bernoulli mixture HMMs (BHMMs) for handwriting word  
398 recognition have been described and improved by the introduction of window  
399 *repositioning* techniques. In particular, we have considered three techniques  
400 of window *repositioning* after window extraction: *vertical*, *horizontal*, and  
401 *both*. They only differ in the way in which extracted windows are shifted to  
402 align mass and window centers (only in the vertical direction, horizontally or  
403 in both directions). In this work, these repositioning techniques have been  
404 carefully described and extensively tested on three well-known databases for  
405 off-line handwriting recognition. In all cases, the best results were obtained  
406 with vertical repositioning. We have reported state-of-the-art results in the  
407 IfN/ENIT database, and also good results on IAM words and RIMES.

408 Our current work is focused on the application of BHMMs to handwrit-  
409 ten text line images and the use of different training techniques. We are also  
410 studying the application of repositioning techniques to other models, par-  
411 ticularly conventional (Gaussian) HMMs. In the mid-term, we plan to try  
412 systems combining our BHMM technology with other technologies such as  
413 Neural Networks.

## 414 Acknowledgment

415 Work supported by the EC (FEDER/FSE), the Spanish MICINN (MIPRCV  
416 “Consolider Ingenio 2010”, iTrans2 TIN2009-14511, MITTRAL TIN2009-  
417 14633-C03-01, erudito.com TSI-020110-2009-439, and a AECID 2010/11 grant).

418 **References**

- 419 Bianne-Bernard, A.L., Menasri, F., Al-Hajj Mohamad, R., Mokbel, C., Ker-  
420 morvant, C., Likforman-Sulem, L., 2011. Dynamic and Contextual In-  
421 formation in HMM Modeling for Handwritten Word Recognition. *IEEE*  
422 *Transactions on Pattern Analysis and Machine Intelligence* 33, 2066–2080.
- 423 Dehghan, M., Faez, K., Ahmadi, M., Shridhar, M., 2001. Handwritten Farsi  
424 (Arabic) word recognition: a holistic approach using discrete HMM. *Pat-*  
425 *tern Recognition* 34, 1057–1065.
- 426 Dreuw, P., Heigold, G., Ney, H., 2009. Confidence-Based Discriminative  
427 Training for Model Adaptation in Offline Arabic Handwriting Recognition,  
428 in: *ICDAR '09, Barcelona (Spain)*. pp. 596–600.
- 429 Giménez, A., Juan, A., 2009. Embedded Bernoulli Mixture HMMs for Hand-  
430 written Word Recognition, in: *ICDAR '09, Barcelona (Spain)*. pp. 896–900.
- 431 Giménez, A., Khoury, I., Juan, A., 2010. Windowed Bernoulli Mixture  
432 HMMs for Arabic Handwritten Word Recognition, in: *ICFHR' 10, Kolkata*  
433 *(India)*. pp. 533–538.
- 434 Grosicki, E., Carré, M., Brodin, J.M., Geoffrois, E., 2009. Results of the  
435 RIMES Evaluation Campaign for Handwritten Mail Processing, in: *IC-*  
436 *DAR '09, Barcelona (Spain)*. pp. 941 –945.
- 437 Grosicki, E., El Abed, H., 2009. *ICDAR 2009 Handwriting Recognition*  
438 *Competition*, in: *ICDAR '09, Barcelona (Spain)*. pp. 1398 – 1402.

- 439 Grosicki, E., El Abed, H., 2011. ICDAR 2011 - French Handwriting Recog-  
440 nition Competition, in: ICDAR '11, Beijing (China). pp. 1459 – 1463.
- 441 Günter, S., Bunke, H., 2004. HMM-based handwritten word recognition: on  
442 the optimization of the number of states, training iterations and Gaussian  
443 components. *Pattern Recognition* 37, 2069–2079.
- 444 Khoury, I., Giménez, A., Juan, A., 2010. Arabic Handwritten Word Recogni-  
445 tion Using Bernoulli Mixture HMMs, in: PICCIT '10, Hebron (Palestine).
- 446 Märgner, V., El Abed, H., 2007. ICDAR 2007 - Arabic Handwriting Recog-  
447 nition Competition, in: ICDAR '07, Curitiba (Brazil). pp. 1274–1278.
- 448 Märgner, V., El Abed, H., 2009. ICDAR 2009 Arabic Handwriting Recogni-  
449 tion Competition, in: ICDAR '09, Barcelona (Spain). pp. 1383–1387.
- 450 Märgner, V., El Abed, H., 2010. ICFHR 2010 - Arabic Handwriting Recog-  
451 nition Competition, in: ICFHR '10, Kolkata (India). pp. 709–714.
- 452 Märgner, V., El Abed, H., 2011. ICDAR 2011 - Arabic Handwriting Recog-  
453 nition Competition, in: ICDAR '11, Beijing (China). pp. 1444 – 1448.
- 454 Marti, U.V., Bunke, H., 2002. The IAM-database: an English sentence  
455 database for offline handwriting recognition. *IJDAR* 5, 39–46.
- 456 Pastor, M., 2007. Aportaciones al reconocimiento automático de texto  
457 manuscrito. Ph.D. thesis. Dep. de Sistemes Informàtics i Computació.  
458 València, Spain.

- 459 Pechwitz, M., Maddouri, S.S., Märgner, V., Ellouze, N., Amiri, H., 2002.  
460 IFN/ENIT - DATABASE OF HANDWRITTEN ARABIC WORDS, in:  
461 CIFED '02, Hammamet (Tunis). pp. 21–23.
- 462 Rabiner, L., Juang, B.H., 1993. Fundamentals of speech recognition.  
463 Prentice-Hall.
- 464 Young, S., et al., 1995. The HTK Book. Cambridge University Engineering  
465 Department.